

Title	High Power Dummy-Load for RF System in the Linac
Author(s)	Shirai, Toshiyuki; Dewa, Hideki; Ego, Hiroyasu; Inoue, Makoto; Iwashita, Yoshihisa; Noda, Akira; Okamoto, Hiromi; Takekoshi, Hidekuni
Citation	Bulletin of the Institute for Chemical Research, Kyoto University (1992), 70(1): 45-54
Issue Date	1992-03-30
URL	http://hdl.handle.net/2433/77433
Right	
Type	Departmental Bulletin Paper
Textversion	publisher

High Power Dummy-Load for RF System in the Linac

Toshiyuki SHIRAI*, Hideki DEWA*, Hiroyasu EGO**, Makoto INOUE*,
Yoshihisa IWASHITA*, Akira NODA*, Hiromi OKAMOTO*
and Hidekuni TAKEKOSHI***

Received February 10, 1992

We have developed a high power dummy-load for the isolator of the RFQ linac. The body of the dummy-load is a modified waveguide and tapers down in order to absorb the RF power effectively. The cemented carbon is used as the RF absorber. The design is based on the transmission line theory. The return loss of the dummy-load is -33.1 dB on a low power measurement and -30.1 dB on a high power test at the RF frequency of 433.3 MHz. It is found that the dummy-load has enough performance for the isolator system.

KEY WORDS : Dummy-load/RF absorber/Circulator/linac

1. INTRODUCTION

In the accelerators, an RF electric field is often used to accelerate charged particles. In our laboratory, the peak RF power of 600 kW is fed to an RFQ linac and an Alvarez linac. The block diagram of the RF system in the linac is shown in Fig. 1^D. A klystron is chosen

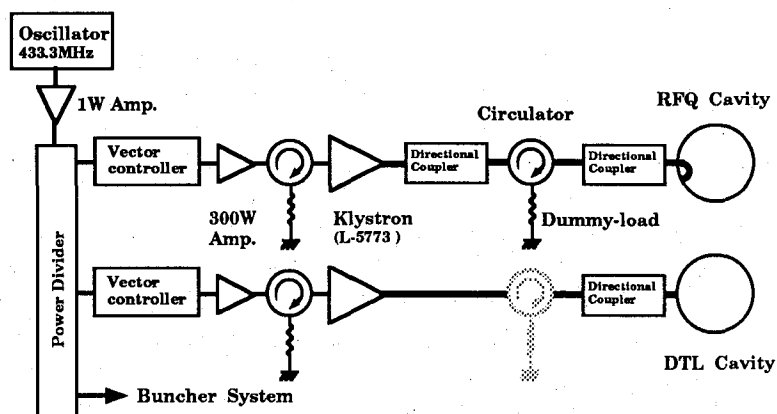


Figure 1. Schematic block diagram of the RF system of the linac.

* 白井敏之, 出羽英紀, 井上 信, 岩下芳久, 野田 章, 岡本宏巳
Nuclear Science Research Facility, Institute for Chemical Research, Kyoto University

** 恵郷博文 : Present address : RIKEN, Wako-shi, Saitama 351-01, Japan.

*** 竹腰秀邦 : Present address : Hiroshima Denki Institute of Technology, Aki-ku, Hiroshima 731-02, Japan.

Table 1. Operating parameters of the RF power source

Klystron	L5773 (Litton)
Frequency	433.3 MHz
Maximum RF power	1.2 MW
Required RF power for linac cavity	600 kW
RF pulse width	60 μ sec
Maximum pulse repetition rate	180 Hz

as a main RF amplifier, because it has high gain and a total RF system can be simple and reliable. The operating parameters of the RF power source are shown in Table 1.

When the power is reflected from the accelerating cavity, the operation of the klystron becomes unstable. So the high power RF isolator has been inserted between the klystron and the RFQ cavity in order to stabilize the operation of the klystron. It also protects the klystron from the reflected power. The isolator is composed of a high power circulator²⁾ and a dummy-load. The reflected power from the cavity is circulated into the dummy-load which absorbs the power. We have developed the dummy-load with the high power handling capability for the isolator. It can be also used in the case of the performance test of the high power RF devices.

We chose a waveguide as a body of the dummy-load and we adopted a forced air cooling. An RF absorber is glued on the inner surface of the dummy-load body. This type dummy-load has an advantage to a coaxial line one by the connectivity because the waveguide (WR 2100) is used as an RF power feeder in our linac system. The water-cooling is more efficient but the forced air cooling is simpler. The present dummy-load was designed so that the forced air cooling could remove the generated heat within the tolerable temperature rise.

In this paper, the design procedure and the performance of the dummy-load is described.

2. DESIGN AND CONSTRUCTION

2-1 RF absorber

The RF absorber should have suitable electric resistivity ($\sim 10 \Omega\text{cm}$) and high heat-resistance. The two materials were tested in this experiment. They are cemented carbon powder and SiC ceramic. The photograph of both the absorbers is shown in Photo 1. The size of the cemented carbon block is $17\text{cm} \times 8\text{cm} \times 1.5\text{cm}$. The cemented carbon has an advantage to have controllable electric resistivity by changing the mixing ratio of the carbon and cement. This advantage is useful to optimize the dummy-load design. It, however, has poor thermal conductivity and the thickness of the RF absorber is limited because of the temperature gradient in it. High heat-resistant cement is used in this absorber.

The SiC ceramic of a honeycomb structure was tested. The weight is lighter and the relative dielectric constant is lower than those of the cemented carbon. The size is $6\text{cm} \times 4\text{cm} \times 4\text{cm}$. It has good thermal conductivity but less controllability of the electric resistivity in a laboratory.

The RF absorber is glued on the inner surface of the dummy-load body by the silicone rubber glue which is heat resistant up to 250°C .

High Power Dummy-Load for RF System in The Linac

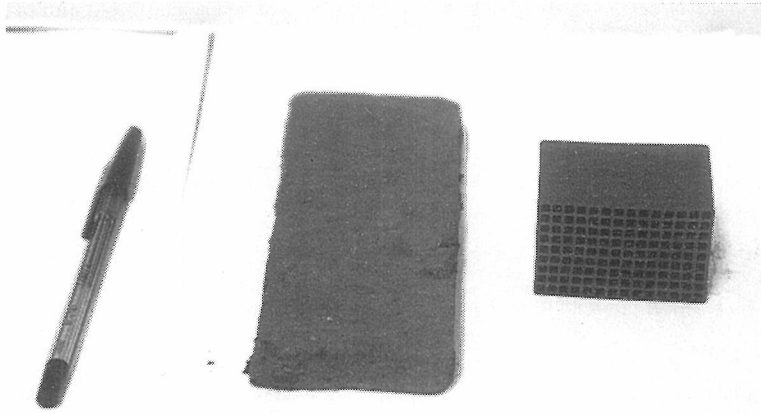


Photo. 1. The photograph of the RF absorbers. The left is the cemented carbon block and the right is the SiC ceramic.

2-2 Design procedure

A schematic view of the dummy-load is shown in Fig. 2. The body of the dummy-load is made of a modified waveguide for an easy connection to the existing waveguide system. The unique feature of the structure is that the height of the body tapers down. For this geometry, the efficiency of the RF absorption is improved than that of straight waveguide body. The body of the dummy-load is divided into four sections, that is, a matching section, a taper section, a flat section and an end section. Each section has a different role described in the following sub sections.

According to the transmission line theory, the input impedance of the dummy-load should be equal to the characteristic impedance of the waveguide for the reflectionless connection.

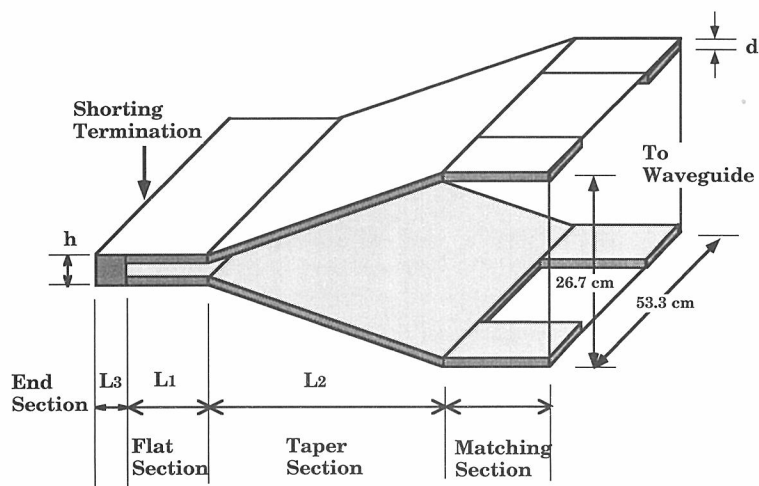


Figure 2. Schematic view of the high power dummy-load.

The dummy-load is designed so that this condition is satisfied. The input impedance of the dummy-load is derived from the characteristic impedance of all sections.

2-2-1 End section

The thick end section is desirable in order to absorb the RF power effectively. The SiC ceramic is used in this section because of its good thermal conductivity.

The characteristic impedance Z_0 of the waveguide is³⁾

$$Z_0 = \frac{\omega \mu_0}{\beta_z}, \quad \beta_z^2 = \omega^2 \varepsilon_0 \mu_0 - \left(\frac{\pi}{a}\right)^2, \quad (1)$$

There ω is an angular frequency of the RF, ε_0 is a dielectric constant of free space and μ_0 is a magnetic permeability of free space. The quantity a is the width of the waveguide. In the end section, the dielectric constant of free space ε_0 is substituted by a complex dielectric constant ε' of the absorber. The characteristic impedance Z_c in this section is given by

$$Z_c = \frac{\omega \mu}{\beta_z}, \quad \beta_z^2 = \omega^2 \varepsilon' \mu_0 - \left(\frac{\pi}{a}\right)^2, \quad \varepsilon' = \varepsilon - i \frac{\sigma}{\omega} \quad (2)$$

where ε is a dielectric constant and σ is an electric conductivity of the absorber.

2-2-2 Flat section

In the flat section, an energy density of the RF is high because its height is low compared to the normal waveguide. Therefore, the efficiency of the RF absorption is high although the RF absorber glued on the wall is thin. The cemented carbon blocks are used as the RF absorber in this section.

From the Maxwell equation in the waveguide, the following equation is obtained,

$$\frac{\partial^2 H_z}{\partial y^2} + \left\{ \omega^2 \varepsilon \mu - \left(\frac{\pi}{a}\right)^2 - \beta_z^2 \right\} H_z = 0 \quad (3)$$

where H_z is the z-component of magnetic field and β_z is the z-component of the propagation constant. Supposed that the solution of this equation is

$$\begin{aligned} H_{z1} &= A \exp(j\beta_{y1}y) + B \exp(-j\beta_{y1}y) & \{0 \leq y < (b-d)\}, \\ H_{z2} &= C \exp(j\beta_{y2}y) + D \exp(-j\beta_{y2}y) & \{y \geq (b-d)\}, \end{aligned} \quad (4)$$

where β_{y1} and β_{y2} are the y-components of the propagation constants and the quantity b is the height of the waveguide. From eqs. (3) and (4), the dispersion relation is

$$\begin{aligned} \omega^2 \varepsilon_1 \mu - \left(\frac{\pi}{a}\right)^2 - \beta_z^2 &= \beta_{y1}^2 & \{0 \leq y < (b-d)\}, \\ \omega^2 \varepsilon_2 \mu - \left(\frac{\pi}{a}\right)^2 - \beta_z^2 &= \beta_{y2}^2 & \{y \geq (b-d)\}, \end{aligned} \quad (5)$$

where ε_1 and ε_2 are complex dielectric constants. The boundary condition of eqs. (3) is

$$\begin{aligned} \frac{\partial H_{z1}}{\partial y} (y=b) &= 0, \\ H_{z1}(y=b-d) &= H_{z2}(y=b-d), \\ \frac{\partial H_{z1}}{\partial y} (y=b-d) &= \frac{\partial H_{z2}}{\partial y} (y=b-d), \\ H_{z2}(y=0) &= 0. \end{aligned} \quad (6)$$

From eqs. (4) and (6), the following relation is obtained

$$\frac{\beta_{y1}}{\omega\varepsilon_1} j \tan(\beta_{y1}d) + \frac{\beta_{y2}}{\omega\varepsilon_2} j \tan\{\beta_{y2}(b-d)\} = 0. \quad (7)$$

From eqs. (5) and (7), the propagation constant β_z is obtained. The characteristic impedance Z_c is

$$Z_c = \frac{\omega\mu}{\beta_z}. \quad (8)$$

2-2-3 Taper section

The height of the flat section is much lower than that of the normal waveguide. This tapered section is installed because a sudden change of the waveguide geometry causes the reflection of the RF power. The characteristic impedance in this section is calculated numerically by the same method as in the flat section with variable quantity b . The cemented carbon blocks are used as the RF absorber in this section.

2-2-4 Matching section

The RF would be reflected at the boundary between the taper section with RF absorber and the normal waveguide by the abrupt impedance change. In this section, the absorber which is the cemented carbon blocks, covers the half of the inner surface area and decrease the total reflection at the boundary (see Fig. 2).

2-3 Numerical calculation

Dividing a transmission line into n sections, the input impedance Z_i at the i -th section is given by following recurrence equation ;

$$Z_i = Z_{ci} \frac{Z_{i-1} + jZ_{ci} \tan(\beta_{zi}L_i)}{Z_{ci} + jZ_{i-1} \tan(\beta_{zi}L_i)} \quad (1 \leq i \leq n), \quad (9)$$

where Z_{ci} is the characteristic impedance, L_i is the length and β_{zi} is the complex propagation

constant in the i -th section. At the end, $Z_0=0$ because the dummy-load is terminated by the shorting plate. The return loss L (dB) is defined as

$$L=10 \log \left(\frac{P_{ref}}{P_{in}} \right), \quad (10)$$

which gives the level of reflection, where P_{in} is the input power of the dummy-load and P_{ref} is the reflected power. The return loss of the dummy-load is calculated by the following relation ;

$$L=20 \log \left(\frac{Z_n - Z}{Z_n + Z} \right), \quad (11)$$

where Z is a characteristic impedance of the waveguide.

Figure 3 shows the dependence of the calculated return loss on the electric resistivity of the cemented carbon block with various geometries. In this calculation, the length of the taper section L_2 is fixed at 90 cm which corresponds to the wavelength in the waveguide. The quantity L_3 is determined to be 4.0 cm and h is limited by the size of available ceramic. The relative dielectric constant of the ceramic is 2.8 and the electric resistivity is 910 Ω cm. The cemented carbon block should be thin to reduce the temperature difference inside. The length of the flat section L_1 is determined so that the reflection would become minimum. As the

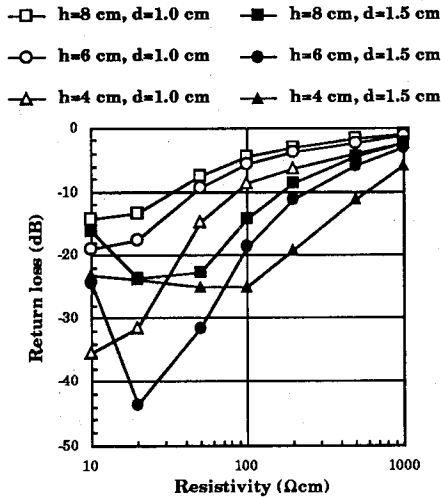


Figure 3. Dependence of the calculated return loss on the electric resistivity of the cemented carbon block with various geometries. The length of the taper section and the end section are fixed at 90 cm and 4.0 cm, respectively.

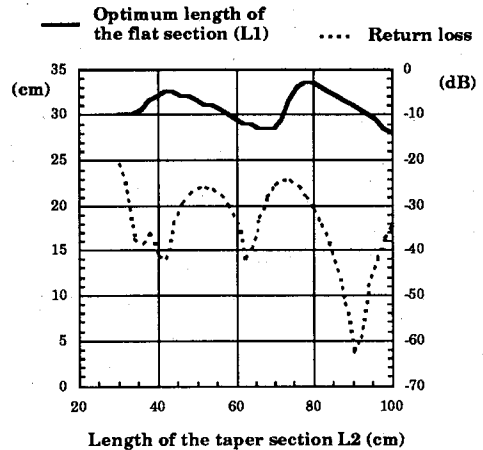


Figure 4. Calculation results of the return loss and the optimum length of L_1 as a function of the taper length L_2 .

results, the following parameters were determined as $d=1.5$ cm, $h=6.0$ cm and the electric resistivity of the cemented carbon block was $20 \Omega\text{cm}$.

The cemented carbon blocks which had been made were found to have higher electric resistivity ($80 \pm 20 \Omega\text{cm}$) than we expected. The relative dielectric constant was about 8.0. Therefore the length of L_1 and L_2 were reoptimized for the RF absorber. Figure 4 shows the return loss and the optimum length of L_1 as a function of the taper length L_2 . The length L_1 and L_2 were determined to be 30 cm and 89 cm, respectively.

2-4 Heat generation

The maximum heat generation is estimated to be about 1 W/cm^2 when the input average power is 10 kW, which corresponds to the peak RF power of 1 MW and the duty factor of 1%.

3. MEASUREMENT SETUP AND RESULTS

3-1 Low power measurement

The return loss is measured at the low RF power level by the standing wave method using the slotted line. The schematic block diagram of the measurement setup is shown in Fig. 5 (a). The standing wave in front of the dummy-load is as follows ;

$$A_{in} e^{jkz} + A_{ref} e^{-jkz} = A_{in} e^{jkz} (1 + \rho e^{j(\theta - 2\beta z)}), \tag{12}$$

where ρ is given by

$$\rho = \left| \frac{A_{ref}}{A_{in}} \right|. \tag{13}$$

A_{in} and A_{ref} are complex amplitudes of the input RF wave and reflected wave, respectively.

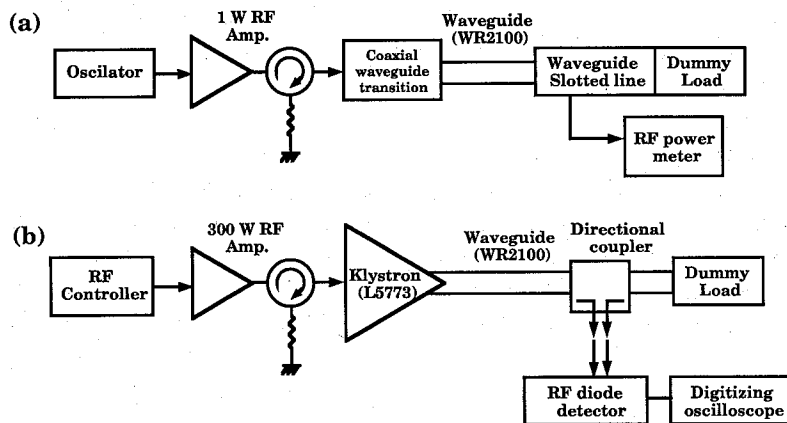


Figure 5. Schematic block diagram of the low power (a) and the high power measurement setup (b) of the return loss of the dummy-load.

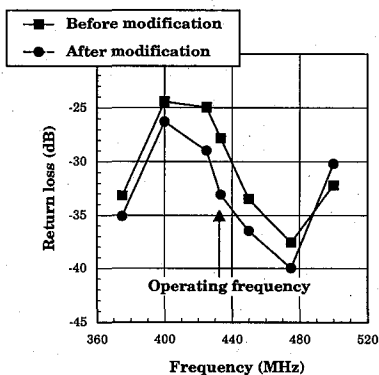


Figure 6. Frequency dependence of the measured return loss at the low power measurement set up.

The quantity θ is a phase difference between the A_{in} and A_{ref} . The quantity β is a propagation constant along the waveguide. The picked up power in the slotted line is proportional to the square of the real part of the expression (12);

$$|A_{in}|^2 \{1 + \rho^2 + 2\rho \cos(\theta - 2\beta z)\}. \quad (14)$$

The measured data are fitted by the expression (14) and the return loss are determined from the quantity ρ .

The squares in Fig. 6 show the frequency dependence of the return loss (before modification). Then, we replaced the ceramic blocks in the end section with the cemented carbon blocks in order to improve the return loss. The return loss is measured at the various thickness L_3 of the end section. After all, the thickness of the end section was changed to be 3.0 cm and the return loss in this condition is shown by solid circles in Fig. 6 (after modification). The return loss became -33.1 dB at the RF frequency of 433.3 MHz after this modification. The measured data is different from the calculation results. It is considered to be caused by the nonuniformity of the cemented carbon material and the approximation used in the characteristic impedance calculation at the taper section.

3-2 High power test

At the high power operation, it is anticipated that the return loss changes from the results of low power measurement because of the temperature rise. The schematic block diagram of the high power test setup is shown in Fig. 5 (b). The input and reflected power of the dummy-load are picked up by the directional coupler which has -60 dB coupling and the signals are monitored by the digitizing oscilloscope (HP 54503A) through the RF diode detectors.

The RF pulse shapes of the input and output power of the dummy-load are shown in Fig. 7 when the input RF power is 900 kW. The dependence of the return loss on the peak RF power level is shown in Fig. 8. The return loss at the peak RF power of 920 kW is -30.1 dB. The power dependence of the return loss is considered to be caused by the harmonics in the

High Power Dummy-Load for RF System in The Linac

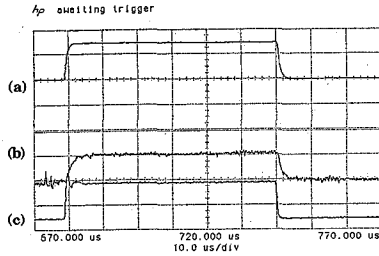


Figure 7. The RF pulse shapes of the input and output power of the dummy-load. The RF frequency is 433.3 MHz. Time base is 10 μ sec/div.
(a) : The input power from the klystron to the dummy-load, 600 kW/div.
(b) : The reflected power from the dummy-load, 1kW/div.
(c) : The input power to the klystron, 50W/div.

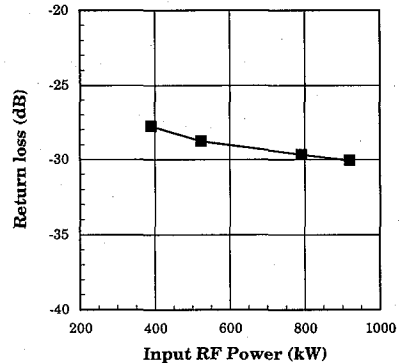


Figure 8. The dependence of the return loss on the peak RF power level. The RF frequency is 433.3 MHz and the duty factor is 1.0%.

output RF power of the klystron.

4. CONCLUSION

We have developed the high power dummy-load based on the transmission line theory. Owing to the tapered waveguide body, the total length is short and the connection becomes easy. The measured return loss of the dummy-load was -30.1 dB at the RF peak power of 920 kW and the duty factor of 1%. At present, the dummy-load is attached to the circulator and is used for the linac operation.

In addition, the performance of the klystron and the circulator was measured with this dummy-load. We confirm that the available output peak power of the klystron is more than 1 MW, which well covers the required power of the accelerating cavity. We also confirm that the isolation of the circulator is more than -25 dB under any condition²⁾. This value is high enough for the isolator system.

ACKNOWLEDGEMENT

The authors would like to thank TOKAI KONETSU KOGYO CO., LTD. who supplied the SiC ceramic. We would like to thank the stuff of Toray Industries, Inc. for their advice about the RF absorber.

T. SHIRAI, H. DEWA, M. INOUE, Y. IWASHITA, A. NODA,
H. OKAMOTO, H. EGO and H. TAKEKOSHI

REFERENCES

- 1) Y Iwashita, et al. ; "System of 7 MeV-Proton Linac", *Bull. Inst. Chem. Res. Kyoto Univ.*, **68**, No. 2 (1990).
- 2) T. Shirai, et al. ; "High power circulator for the 433.3 MHz proton linac", *Nucl. Instr. and Meth.* Submitted.
- 3) H. A. ATWATER, "Introduction to Microwave Theory", McGraw Hill (1962).